

<https://helda.helsinki.fi>

Photometric study for near-Earth asteroid (155140) 2005 UD

Huang, J.-N.

2021-01

Huang , J-N , Muinonen , K , Chen , T & Wang , X-B 2021 , ' Photometric study for near-Earth asteroid (155140) 2005 UD ' , Planetary and Space Science , vol. 195 , 105120 . <https://doi.org/10.1016/j.pss.2020.105120>

<http://hdl.handle.net/10138/352238>

<https://doi.org/10.1016/j.pss.2020.105120>

cc_by_nc_nd

acceptedVersion

Downloaded from Helda, University of Helsinki institutional repository.

This is an electronic reprint of the original article.

This reprint may differ from the original in pagination and typographic detail.

Please cite the original version.



Contents lists available at ScienceDirect

Planetary and Space Science

journal homepage: www.elsevier.com/locate/pss

Photometric study for near-Earth asteroid (155140) 2005 UD

J.-N. Huang^{a,b,c}, K. Muinonen^{d,e}, T. Chen^f, X.-B. Wang^{a,b,c,*}^a Yunnan Observatories, Chinese Academy of Sciences, Kunming, 650216, China^b School of Astronomy and Space Sciences, University of Chinese Academy of Sciences, Beijing, 100049, China^c Key Laboratory for Structure and Evolution of Celestial Objects, CAS, Kunming, 650216, China^d Department of Physics, University of Helsinki, Gustaf Hällströmin katu 2, P.O. Box 64, FI-00014 U, Helsinki, Finland^e Finnish Geospatial Research Institute, Geodeetinrinne 2, FI-02430, Masala, Finland^f Corona Borealis Observatories, Ali, China

ARTICLE INFO

Keywords:

Near-earth-asteroid

Photometry

Shape inversion

Phase function

ABSTRACT

The Apollo-type near-Earth asteroid (155140) 2005 UD is thought to be a member of the Phaethon-Geminid meteor stream Complex (PGC). Its basic physical parameters are important for unveiling its origin and its relationship to the other PGC members as well as to the Geminid stream. Adopting the Lommel-Seeliger ellipsoid method and H , G_1 , G_2 phase function, we carry out spin, shape, and phase curve inversion using the photometric data of 2005 UD. The data consists of 11 new lightcurves, 3 lightcurves downloaded from the Minor Planet Center, and 288 sparse data points downloaded from the Zwicky Transient Facility database. As a result, we derive the pole solution of $(285^\circ.8^{+1.1}_{-5.3}, -25^\circ.8^{+5.3}_{-12.5})$ in the ecliptic frame of J2000.0 with the rotational period of $5.2340^{+0.00004}_{-0.00001}$ h. The corresponding triaxial shape (semiaxes $a > b > c$) is estimated as $b/a = 0.76^{+0.01}_{-0.01}$ and $c/a = 0.40^{+0.03}_{-0.01}$. Using the calibrated photometric data of 2005 UD, the phase function parameters H , G_1 , G_2 are estimated as $17.22^{+0.03}_{-0.03}$ mag, $0.61^{+0.02}_{-0.02}$, and $-0.006^{+0.006}_{-0.006}$, respectively. Correspondingly, the phase integral q , photometric phase coefficient k , and the enhancement factor ζ are 0.2508, -1.9224 , and 1.6642. From the values of G_1 and G_2 , 2005 UD is likely to be a C-type asteroid. We estimate the equivalent diameter of 2005 UD from the new H -value: it is 1.28 ± 0.02 km using its new geometric albedo of 0.14.

1. Introduction

Near-Earth asteroids (NEAs) derive from the main belt of asteroids and are composed of planetesimal material remaining from the early stages of the Solar System. They contain important information about the Solar System's formation and evolution. Thus, the physical study for NEAs can allow us to know more about the history of the Solar System, including that of the asteroids. Apollo-type near-Earth asteroid 2005 UD is discovered by the Catalina Sky Survey in October 22, 2005. Together with (3200) Phaethon and 1996 YC, the three of them constitute comprise the Phaethon-Geminid stream Complex, briefly PGC. Ohtsuka et al. (2006) investigated the orbital evolution of 2005 UD and Phaethon, and suggested the object may be a split nucleus of Phaethon. As a member of PGC, the physical properties of 2005 UD should provide information about its origin and relationship to the other PGC members and to the Geminid meteors.

Several groups have carried out physical studies of 2005 UD. Ohtsuka et al. (2006) inferred that 2005 UD is a km-size object. Jewitt and Hsieh

(2006)'s data of 2005 UD showed a periodic brightness variation of 5.2492 h with an amplitude of 0.4 mag. They also estimated the diameter of 2005 UD to be 1.3 ± 0.1 km, assuming a geometric albedo of 0.11 (the geometric albedo of Phaethon). Kinoshita et al. (2007) determined the rotation period for 2005 UD, as 5.23 h with an amplitude of 0.44 ± 0.02 mag, and their multi-band photometric observations suggested that 2005 UD is of F or B type. Later, Kasuga and Jewitt (2008) suggested that 2005 UD is a C-type asteroid, based on the color index. Kasuga and Jewitt (2008) determined the absolute magnitude of 2005 UD to be 17.23 ± 0.03 mag, and derived a diameter of 1.2 ± 0.1 km, assuming an albedo of 0.11. Jewitt (2013) re-determined the surface color indices of 2005 UD and estimated its absolute magnitude to be 17.08 mag, assuming a slope of $G = 0.15$. Based on the WISE observations, Masiero et al. (2019) determined the geometric albedo of 2005 UD to be 0.14 ± 0.09 , and derived a diameter of 1.2 ± 0.4 km. Recently, Krugly et al. (2019) and Warner and Stephens (2019) reported a similar rotation period for 2005 UD. Krugly et al. (2019) determined the linear phase-angle coefficient of 0.043 mag deg^{-1} . As for the spin and shape parameters, there is no

* Corresponding author. Yunnan Observatories, Chinese Academy of Sciences, Kunming, 650216, China.,

E-mail addresses: wangxb@ynao.ac.cn, huangjianing@ynao.ac.cn (X.-B. Wang).

<https://doi.org/10.1016/j.pss.2020.105120>

Received 6 February 2020; Received in revised form 17 October 2020; Accepted 19 October 2020

Available online xxx

0032-0633/© 2020 Elsevier Ltd. All rights reserved.

Table 1
Information on the photometric observations of near-Earth asteroid 2005 UD.

Date	r	Δ	α	Mag-V	Filter	N	Data source
(UT)	(au)	(au)	(deg)				
2018/10/05	1.229	0.250	21.301	15.9	C	135	<i>Ourdata</i>
2018/10/06	1.242	0.258	17.588	15.9	C	229	<i>Ourdata</i>
2018/10/07	1.258	0.268	14.198	15.9	C	263	<i>Ourdata</i>
2018/10/10	1.296	0.300	5.671	15.8	R	36	<i>Ourdata</i>
2018/10/11	1.309	0.311	3.152	15.8	V, R	227	<i>Ourdata</i>
2018/10/12	1.321	0.323	1.790	15.7	C	52	R, <i>Stephens</i>
2018/10/12	1.321	0.323	0.964	15.7	V	204	<i>Ourdata</i>
2018/10/13	1.335	0.337	1.726	15.7	V	290	<i>Ourdata</i>
2018/10/14	1.346	0.349	3.685	15.8	V	292	<i>Ourdata</i>
2018/10/15	1.354	0.358	4.642	16.0	C	132	R, <i>Stephens</i>
2018/10/15	1.359	0.364	5.414	16.1	R	180	<i>Ourdata</i>
2018/10/16	1.365	0.372	6.455	16.3	C	116	R, <i>Stephens</i>
2018/10/16	1.371	0.378	7.130	16.5	R	182	<i>Ourdata</i>
2018/10/17	1.384	0.393	8.827	16.6	R	208	<i>Ourdata</i>
2017/11/16–2019/11/30						288	<i>ZTF^{Facility}</i>

Note that r and Δ are heliocentric and topocentric distances of the asteroid, α is the solar phase angle, Mag-V is the mean of the observed V-band magnitudes in a night, N is the number of data points, and *ZTF^{Facility}* refers to IRSA, Spitzer, WISE, Herschel, Planck, SOFIA, IRTF, IRAS, and MSX.

further information preceding our study.

For understanding the physical properties of 2005 UD, we carried out 11 nights of photometric observations in 2018. In addition, we downloaded the photometric data of 2005 UD from the Zwicky Transient Facility (ZTF) and Minor Planet Center (MPC) databases. ZTF is a robotic time-domain astronomical sky survey. The small Solar System bodies are important targets of the survey. In total, 288 data points of 2005 UD are downloaded from the ZTF database.

In the article, we present our new photometric observations of 2005 UD and the photometric analyses results with the inverse methods based on the Lommel-Seeliger ellipsoids model (Muinonen et al. (2015)) and H , G_1 , G_2 phase function (Muinonen et al. (2010)). Therefore, Sect. 2 are information on observations and data reductions for the object, Sect. 3 shows the methods of lightcurve inversion and phase curve inversion, together with the results and discussion. In the last section, a summary is presented.

2. Observations and data reductions

We obtained 11 nights of photometric observations of 2005 UD in October 2018 using a 30-cm telescope and a 3326×2504 CCD of the Corona borealis observatory (code N55) at Ali of Tibet, China. The field of view (FOV) of the CCD is $28'.4 \times 21'.4$. The data were gathered through C (Clear), R, or V filters depending on the weather conditions and the signal-to-noise ratio. Additional observational information is shown in Table 1. During the photometric observations, sidereal tracking and short exposure times were utilized. Because of fast projected movement in sky plane of 2005 UD in the periods of observations, ($8''.7 \sim 3''.5/\text{min}$), the telescope pointing was shifted once or twice in some nights to keep the object in the FOV.

The photometric images were reduced according to the standard procedures with the IRAF software. The effects of bias, flat field, and dark current were corrected first. The cosmic rays in the images were removed properly. The magnitudes of the celestial objects in the scientific frames were measured using the Apphot task of IRAF with an optimum aperture. We tried 3–5 apertures ranging 2.0–2.3 times the full width at half maximum (FWHM) to find the optimum aperture, which gives the

minimum dispersion of the lightcurve.

Some systematic errors in the photometric data, related to atmospheric extinction and temporal or positional changes of stars in the CCD, were simulated with the aid of reference stars in the images using the coarse de-correlation method (Collier Cameron et al. (2006); Wang et al. (2013)) and the SYSREM method (Tamuz et al. (2005)). The former performs a coarse initial de-correlation by referencing each star's magnitude to its own mean, finding small night-to-night and frame-to-frame differences in the zero point. After the coarse de-correlation, the reduced magnitudes of celestial objects can be derived (see Eq. (1d) below) by removing the biases due to the objects' mean magnitude in each night and zero-point in each frame. The latter method simulates the low-level systematic errors in the reduced magnitudes by those chosen reference stars. Then those simulated low-level errors, or, say, patterns in the reduced magnitudes are removed from the reduced magnitudes of the 2005 UD. The ratio of signal to noise of the lightcurves (reduced magnitudes in one night) is therefore enhanced. The time stamp of each observation of the asteroid is corrected for the light travel time. The distance effects on the asteroid's magnitude are also corrected by the formula $-5 \log(r\Delta)$. In total, 2206 data points were obtained in 11 nights. For the aim of shape inversion, the relative intensities of 2005 UD are used, which are derived by normalizing the mean intensity of each lightcurve to unity.

For the phase curve analysis of 2005 UD, photometric data obtained in different nights and/or with different filters need to be converted into the same photometric system, e.g., the standard V-band magnitudes. In this work, we firstly transformed the instrumental magnitudes of celestial objects into the r' band of the Carlsberg Meridian Catalogue 15 (CMC15). The relationship between the instrumental magnitude and the r' -band of CMC15 (Eq. (2)) is derived by the reference stars in the images. The reference stars are chosen based on a threshold in the intrinsic variance, e.g., 0.01 mag in the case of 2005 UD's observations. The intrinsic variance of the stars $\sigma_{s(i)}$ in a night and the variance of the observations $\sigma_{i(j)}$ (the variance of reference stars' magnitudes in an image after removing their means), are output by the coarse de-correlation method (for details, see Collier Cameron et al. (2006)). Briefly, the two variances above are estimated iteratively by minimizing the value of χ^2 (Eq. (1a) below), providing zero points of the stars' magnitudes \hat{M}_i in a night and the zero point of each frame \hat{Z}_j (calculated with Eqs. (1b) and (1c)). The quantities \hat{M}_i and \hat{Z}_j are re-computed when we have new values for $\sigma_{s(i)}$ and $\sigma_{i(j)}$. The iterative procedure is ended when the four quantities no longer change significantly. For a given reference star i , the reduced magnitudes r_{ij} in a night, j denoting the index of a frame, are close to random, essentially realizations of white noise. The following equation gives a mathematical description of the procedures outlined above:

$$\chi^2 = \sum (m_{ij} - \hat{M}_i - \hat{Z}_j)^2, \quad (a)$$

$$\hat{M}_i = \frac{\sum_j (m_{ij} - \hat{Z}_j) w_{ij}}{\sum_j w_{ij}}, \quad w_{ij} = \frac{1}{\sigma_{ij}^2 + \sigma_{s(i)}^2}, \quad (b)$$

$$\hat{Z}_j = \frac{\sum_i (m_{ij} - \hat{M}_i) u_{ij}}{\sum_i u_{ij}}, \quad u_{ij} = \frac{1}{\sigma_{ij}^2 + \sigma_{s(i)}^2}, \quad (c)$$

$$r_{ij} = m_{ij} - \hat{M}_i - \hat{Z}_j. \quad (d)$$

Here m_{ij} represents the observed magnitude of star i in frame j , and σ_{ij} is the corresponding observational uncertainty.

The magnitude zero points of selected reference stars in a night \hat{M}_i are applied to fit the relationship of Eq. (2):

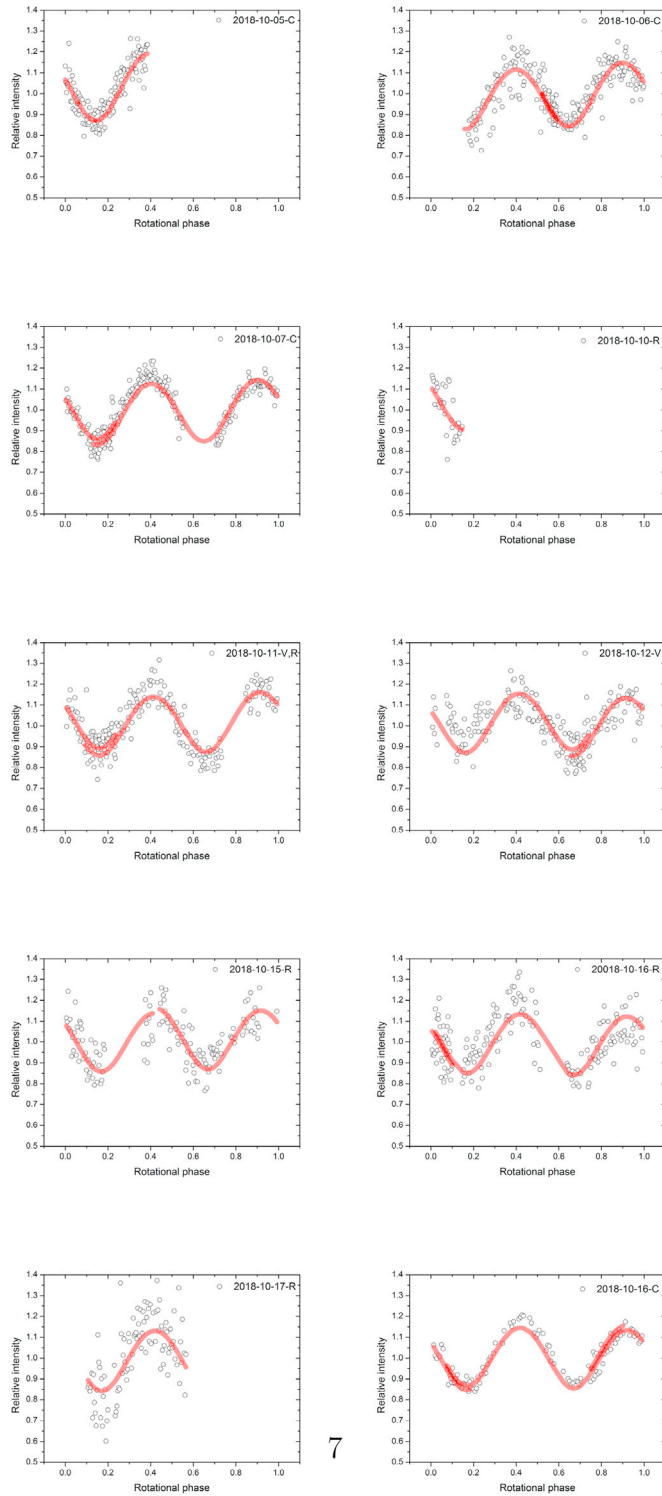


Fig. 1. Ten lightcurves of 2005 UD folded with the period of 5.2340 h. Red lines are best-fit model values. (For interpretation of the references to color in this figure legend, the reader is referred to the Web version of this article.)

$$\hat{M}_i = M_0 + M_{(r')_i} + k \times (J_i - K_s) \quad (2)$$

In detail, the parameters M_0 and the coefficient k in Eq. (2) are fitted by comparing the \hat{M}_i values of selected stars to their values $M_{(r')_i}$ in CMC15. The color indices $(J_i - K_s)$ of reference stars come from the 2MASS catalogue. The r' -band of CMC15 is the same as that in the Sloan Digital Sky Survey. Using the derived parameters M_0 and k , the mean

magnitude of the asteroid in a given night is transformed into the r' -band of the CMC15 photometric system, denoted by $M(r')_{ast}$. For no measurement value for 2005 UD's color index $(J - K_s)_{ast}$, we temporally use the value of Phaethon's 0.275.¹ Then the r' -band magnitudes of the asteroid are converted into the standard V-band magnitude by another linear relationship (Dymock and Miles (2009)):

$$V_{ast} = 0.6278 \times (J - K_s)_{ast} + 0.9947 \times M(r')_{ast} \quad (3)$$

The calibrated mean magnitudes V_{ast} of each lightcurves of 2005 UD are used in the phase curve inversion: the results are shown in Fig. 2. The individual data points of the asteroid in a night are calibrated by adding the calibrated mean magnitude V_{ast} into the reduced magnitudes in that night.

Besides our new data, we downloaded, from the MPC Asteroid Lightcurve Photometry Database,² three dense lightcurves of 2005 UD observed on 12, 15, and October 16, 2018. These data have been converted into the V-band.

Also, we downloaded 288 sparse photometric data of 2005 UD from the ZTF Data release.³ The ZTF is a robotic time-domain sky survey using the Samuel Oschin 48-inch Schmidt telescope with a new Mosaic CCD of a 47 square-degree FOV. This observational system is equipped with three filters: ZTF-g, ZTF-r, and ZTF-i. The ZTF data reduction follows the data processing system of the Palomar Transient Factory (PTF) survey. They use a fixed aperture of 8 pixels to obtain instrumental magnitudes and carry out photometric calibration with the reference stars in the SDSS catalogue and in the ZTF images (Ofek et al. (2012); Laher et al. (2014); Bellm et al. (2019)). The downloaded 288 photometric data of 2005 UD have been converted into the mean standard V band (Ofek et al. (2012); Bellm et al. (2019)).

For all downloaded data, we have corrected the distance effects on the magnitude and light travel time in the recorded time stamps (see Fig. 2).

3. Photometric analysis

3.1. Lommel-Seeliger ellipsoid model

For a spheroid asteroid, the observed brightness at a time is related to surface scattering properties, size of asteroid and the observation geometry. The brightness of the asteroid varies only with the solar phase angle. For a nonspherical asteroid, the irregular shape causes the additional variation of brightness during its rotation. In this case, the brightness model of asteroid involves a shape model and a surface scattering law.

The regular shape of lightcurves of 2005 UD (Fig. 1) with two peaks implies a regular shape of the asteroid. The Lommel-Seeliger scattering law is suit for weakly scattering surface of asteroids. That is the main reason why we use, in the lightcurve inversion, the triaxial ellipsoid model with the Lommel-Seeliger scattering law (LS ellipsoid; Muinonen et al. (2015)). For an elementary facet dA on the asteroid's surface, the brightness of the facet with the Lommel-Seeliger law can be written as

$$dL = \frac{1}{4} F_0 \mu_0 \omega_0 P(\alpha) \frac{1}{\mu + \mu_0} \mu dA, \quad (4)$$

where πF_0 is the incident solar flux on the facet, ω_0 is the single-scattering albedo, α is the solar phase angle, and $P(\alpha)$ is the single-scattering phase function.

The integrated brightness of an ellipsoid asteroid with the Lommel-Seeliger scattering law (Muinonen et al. (2015)) is given as

¹ <https://sbnapps.psi.edu/ferret/SimpleSearch/results.action>.

² http://alcddef.org/PHP/alcddef_GenerateALCDEFPage.php

³ <https://irsa.ipac.caltech.edu/applications/ztf/>.

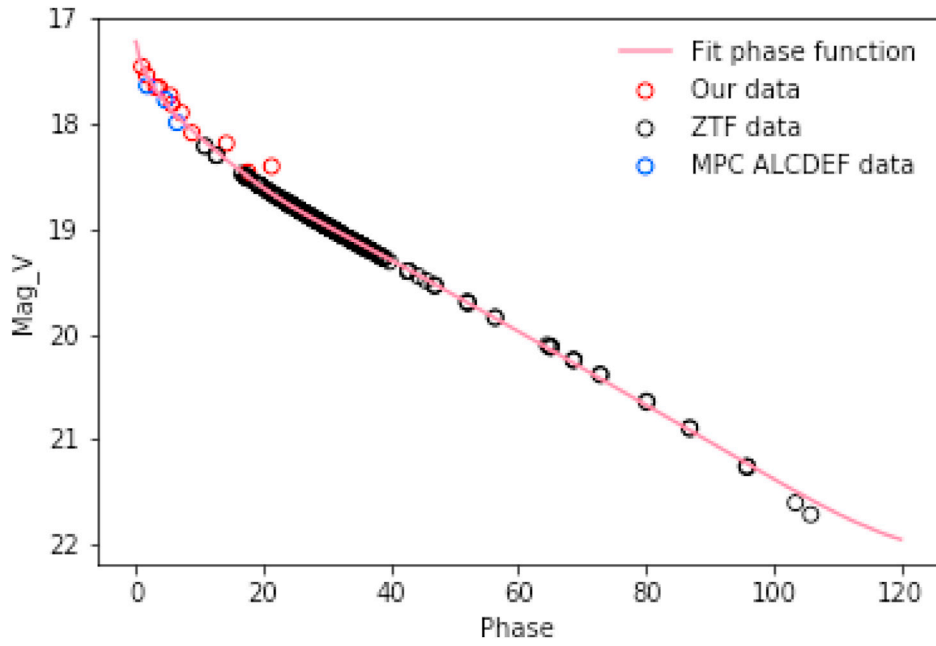


Fig. 2. Phase curve of 2005 UD.

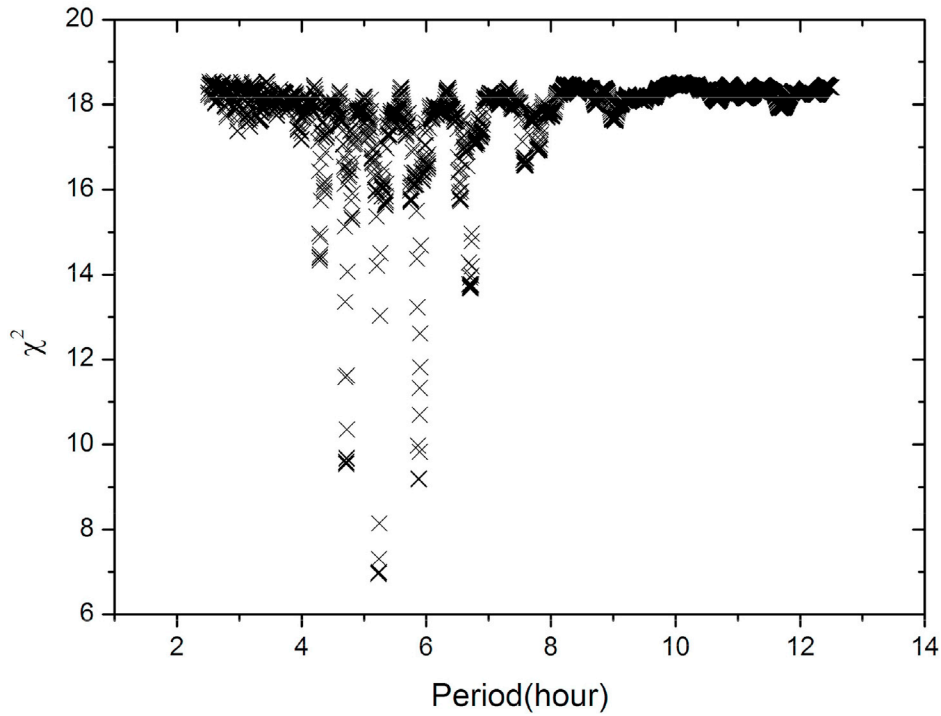


Fig. 3. χ^2 -values versus trial periods.

$$L(\alpha, e_{\odot}, e_{\oplus}) = \frac{1}{8} \pi F_0 abc \varpi_0 P(\alpha) \frac{S_{\odot} S_{\oplus}}{S} \left\{ \cos(\lambda' - \alpha') + \cos \lambda' + \sin \lambda' \sin(\lambda' - \alpha') \times \ln \left[\cot \frac{1}{2} \lambda' \cot \frac{1}{2} (\alpha' - \lambda') \right] \right\} \quad (5)$$

Using the relationship

$$\frac{1}{8} \varpi_0 P(\alpha) = p \frac{\phi_{HG_1, G_2}(\alpha)}{\phi_{LS}(\alpha)},$$

Eq. (5) can be re-written as

$$L(\alpha, e_{\odot}, e_{\oplus}) = \pi F_0 abc p \frac{\phi_{HG_1, G_2}(\alpha)}{\phi_{LS}(\alpha)} \frac{S_{\odot} S_{\oplus}}{S} \left\{ \cos(\lambda' - \alpha') + \cos \lambda' + \sin \lambda' \sin(\lambda' - \alpha') \times \ln \left[\cot \frac{1}{2} \lambda' \cot \frac{1}{2} (\alpha' - \lambda') \right] \right\}, \quad (6)$$

Here, e_{\odot} and e_{\oplus} denote the unit vectors of solar and viewer directions, a , b , and c are the three semimajor axes of the ellipsoid, and the auxiliary quantities S_{\odot} , S_{\oplus} , α' , λ' are functions of the illumination and viewing geometry, pole orientation, and shape of the asteroid. For details, the reader is referred to Eqs. 11 and 12 in Muinonen et al. (2015).

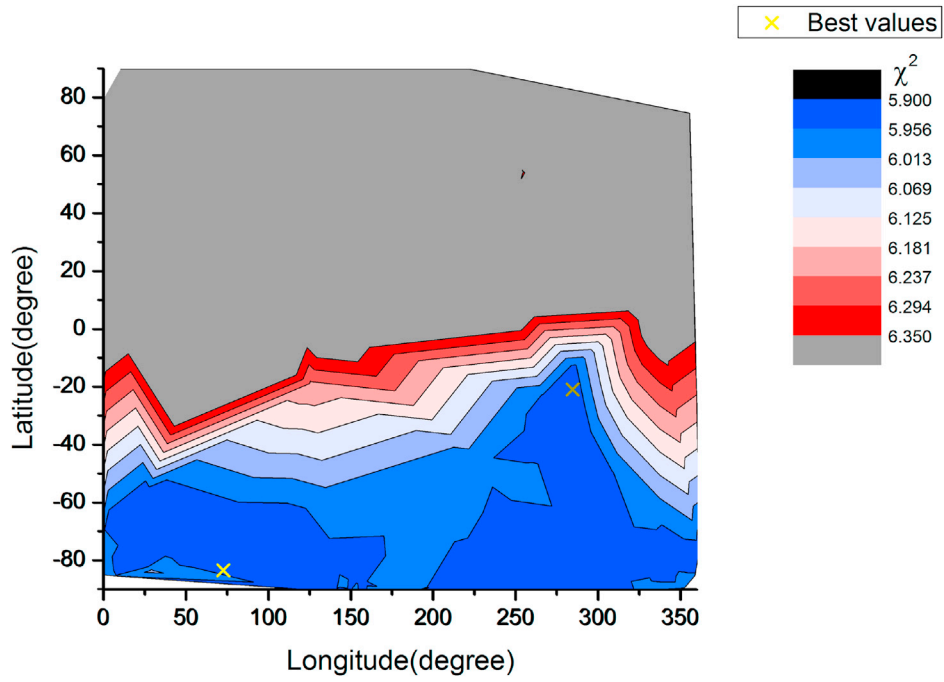


Fig. 4. χ^2 -values versus trial pole orientations.

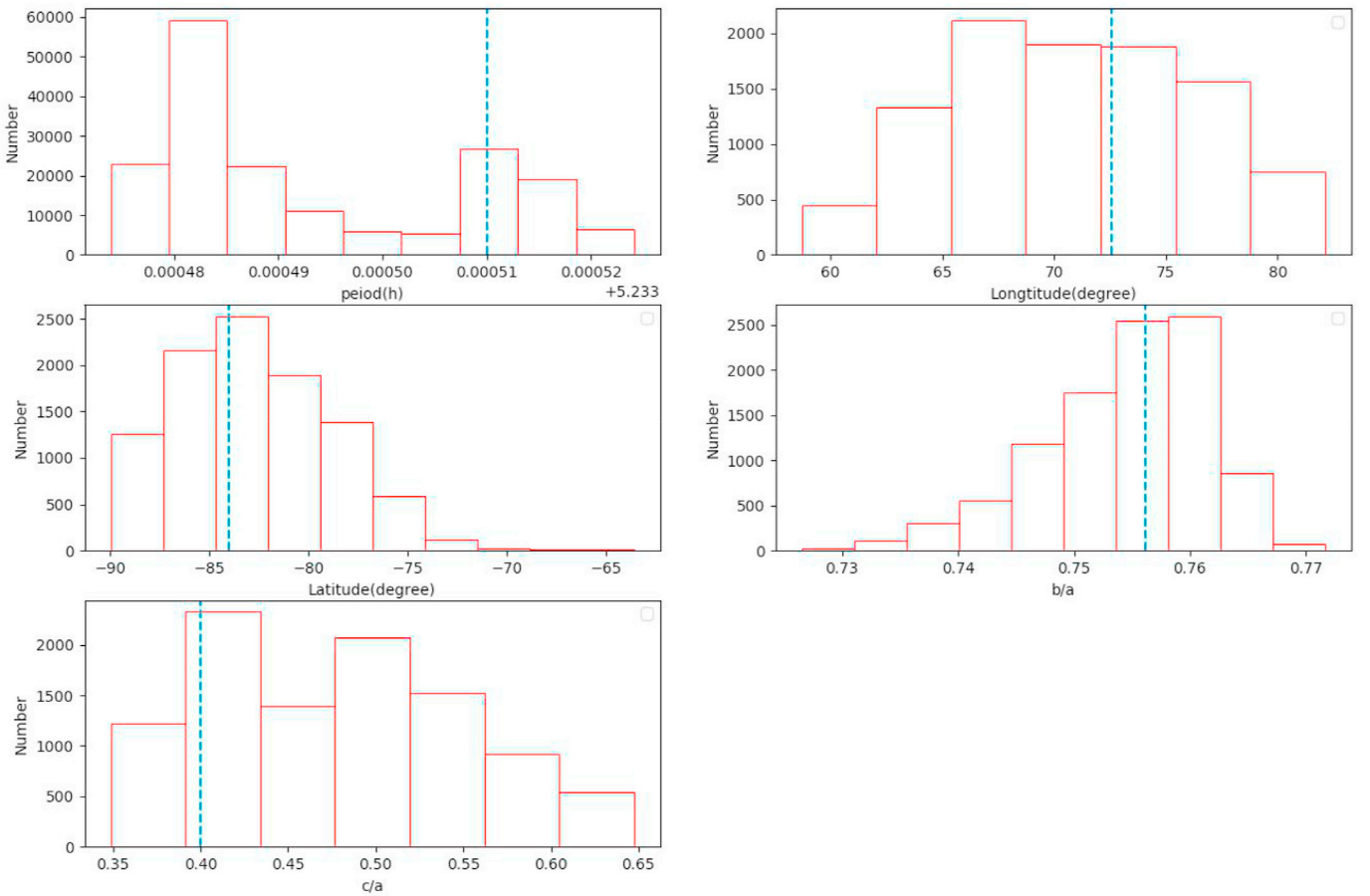


Fig. 5. Joint distributions of spin and shape parameters for Pole 1.

where

$$\phi_{LS}(\alpha) = 1 - \sin \frac{1}{2} \alpha \tan \frac{1}{2} \alpha \ln \left(\cot \frac{1}{4} \alpha \right).$$

$\phi_{LS}(\alpha)$ is the Lommel-Seeliger disk-integrated phase function for a spherical asteroid and p is the geometric albedo. In the model above, the H, G_1, G_2 phase function (Muinonen et al. (2010)) is incorporated into the LS-ellipsoid brightness model.

In short, altogether 12 unknown parameters are involved in the LS-ellipsoid model. They are the rotational period Per , pole orientation (λ, β) in the ecliptic frame of J2000.0, rotational phase φ_0 at epoch JD_0 , three semimajor axes (a, b, c), geometric albedo p , phase function parameters H, G_1, G_2 , and the equivalent diameter of asteroid D . To derive the solution of those unknown parameters, the flexible Nelder-Mead downhill method and a Markov-chain Monte Carlo method (MCMC) are applied in our photometric analysis procedure. In practice, the analysis procedure of 2005 UD consists of two parts: the shape inversion of 2005 UD with the LS-ellipsoid model and the phase curve inversion. In the first part, we estimate rotation period, pole longitude and latitude, and three semimajor axes using 14 dense lightcurves. In the second part, using calibrated photometric data of 2005 UD, the phase curve parameters H, G_1, G_2 are retrieved.

3.2. Shape inversion

Altogether 14 dense lightcurves of 2005 UD are used to invert the spin and shape parameters by the Nelder-Mead downhill simplex method. Furthermore, the uncertainties of the parameters are assessed by the MCMC method.

Using the downhill simplex least-squares method, the following

$\chi^2(Par)$ is minimized:

$$\chi^2(Par) = \sum_{i=1}^{N_0} \sum_{j=1}^{N_i} \frac{1}{\sigma_{ij}^2} [L_{obs,ij} - L_{ij}(Par)]^2. \quad (7)$$

In practical shape inversion with Eq. (7), only 7 parameters ($Per, \lambda, \beta, \varphi_0, a, b, c$) are estimated and the rest of the parameters are kept fixed. Here N_0 is the number of lightcurves used, N_i is the number of data points in the i th lightcurve, $L_{obs,ij}$ is the j th observed data point in the i th lightcurve, and σ_{ij} is its corresponding uncertainty. $L_{ij}(Par)$ is the modeled brightness calculated with the LS-ellipsoid model.

To find the most probable rotation period, a wide range of periods within 2.5–12.5 h was scanned with a step of $Per^2/2T$ (here Per is the assumed period and T is the time span of all involved data). During each step of period scanning, hundreds of different initial poles distributed uniformly over the unit sphere are tested. Fig. 3 shows the χ^2 of the lightcurve fitting versus the trial period, the most likely value of period is located at 5.2338 h. Secondly, we scanned the entire unit sphere with a step of 1° in longitude and latitude directions to find the most probably pole of 2005 UD using the period of 5.2338 h as the initial value. The contours of χ^2 versus the trial poles are shown in Fig. 4. The areas in dark blue in Fig. 4 are corresponding to relatively small χ^2 . Two candidate poles of $(73^\circ, -84^\circ)$ and $(285^\circ, -21^\circ)$ are found with almost equal values of χ^2 (yellow crosses in Fig. 4). Taking the scanned spin parameters as initial values, unknown parameters are resolved with the Nelder-Mead downhill simplex method. Finally, we arrive at the following pair of pole solutions: Pole 1 at $(72^\circ.6, -84^\circ.6)$ with axial ratios of $b/a = 0.76, c/a = 0.40$ and Pole 2 at $(285^\circ.8, -25^\circ.8)$ with axial ratios of $b/a = 0.76$ and $c/a = 0.40$. The periods corresponding to the poles are close to 5.2338 h.

In order to derive the uncertainties for the spin and shape parameters

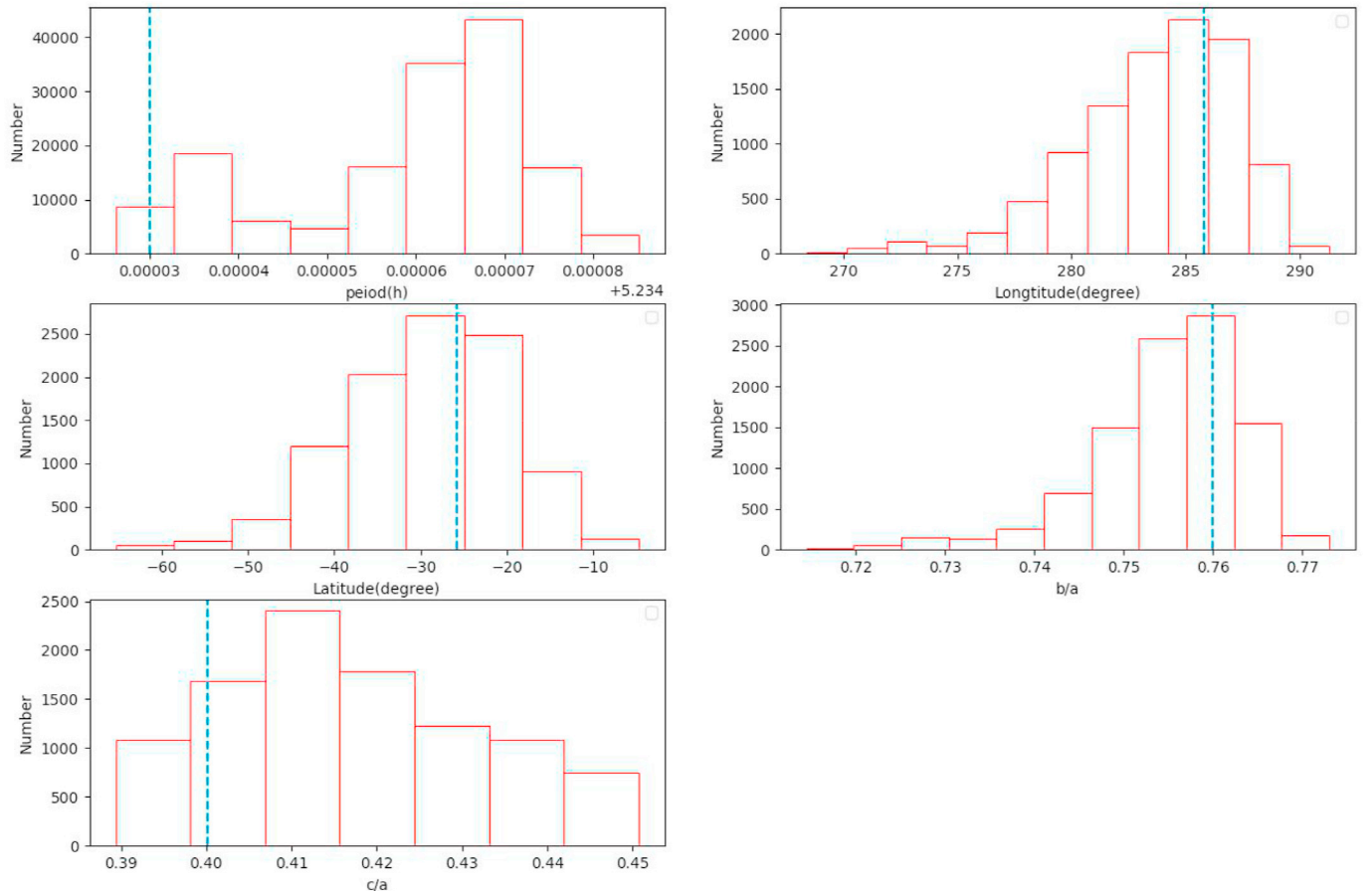


Fig. 6. Joint distributions of spin and shape parameters for Pole 2.

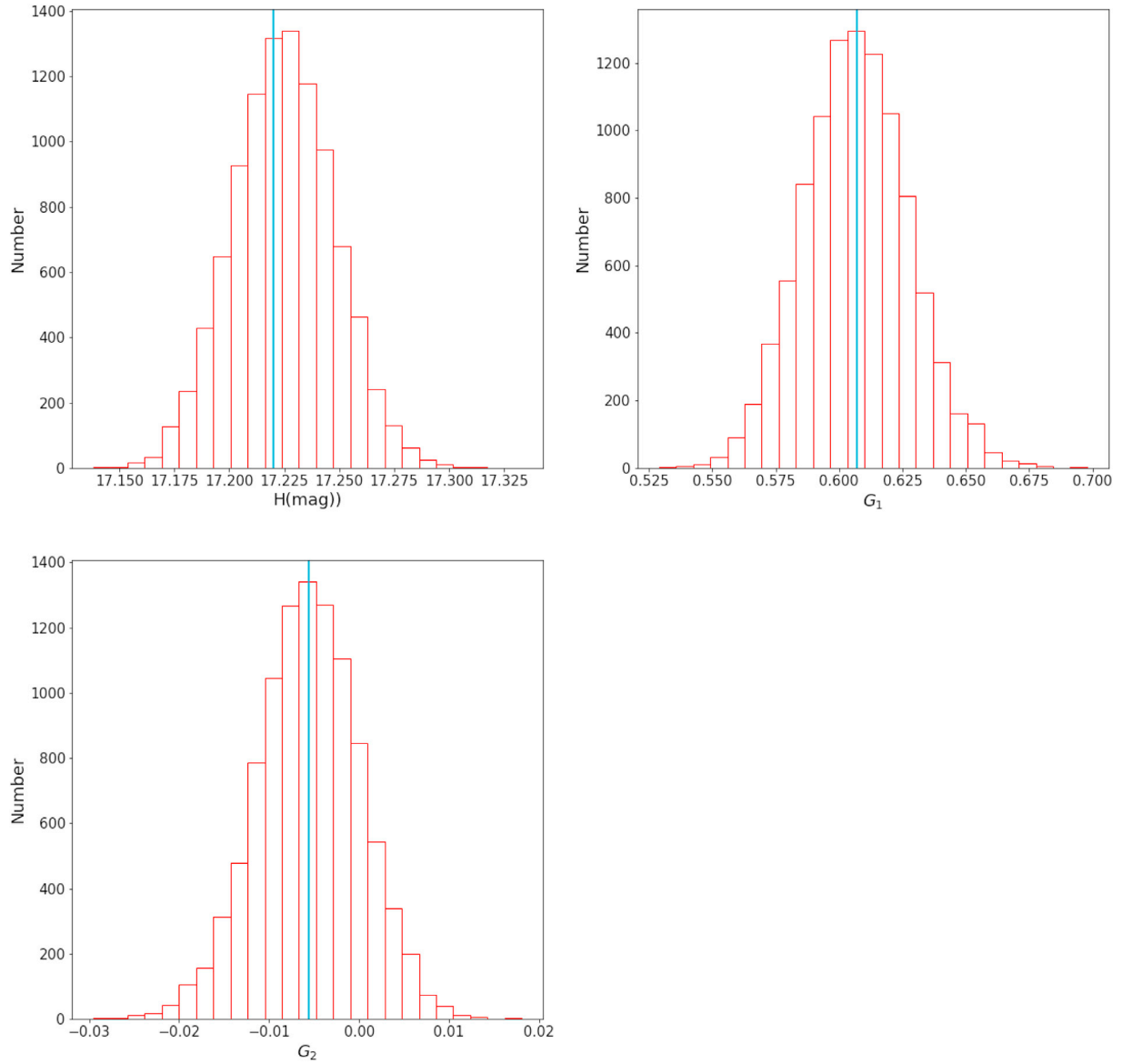


Fig. 7. Joint distributions of H , G_1 , G_2 for 2005 UD.

of 2005 UD, the virtual-observation MCMC method is applied in the lightcurve inversion of 2005 UD (Muinonen et al. (2015)). The a posteriori probability density for the parameters is obtained by a Metropolis-Hastings sampling from the proposal densities of the parameters which are of virtual least-squares solutions derived from virtual photometric data. The virtual photometric data are generated by adding Gaussian noise into the observations. At least 10000 samples are obtained with the MCMC simulation. The joint distributions of the spin parameters are shown in Fig. 5 for Pole 1 and Fig. 6 for Pole 2. The dotted lines in Figs. 5 and 6 are the best-fit values of the parameters. The intervals between the best-fit value and the $1 - \sigma$ limits for each distribution are used to estimate the uncertainties of the parameters. For 2005 UD, the best-fit values of the parameters with their uncertainties are as follows: Pole 1 at $(72^\circ.6^{+4.2}_{-7.3}, -84^\circ.6^{+6.2}_{-2.1})$ with axial ratios $b/a = 0.75^{+0.01}_{-0.01}$ and $c/a = 0.40^{+0.16}_{-0.01}$ and Pole 2 at $(285^\circ.8^{+1.1}_{-5.3}, -25^\circ.8^{+5.3}_{-12.5})$ with axial ratios $b/a = 0.76^{+0.01}_{-0.01}$ and $c/a = 0.40^{+0.03}_{-0.01}$. The periods corresponding to the poles are $5.23351^{+0.00002}_{-0.00001}$ h and $5.23403^{+0.00004}_{-0.00001}$ h, respectively. Comparing the distributions of the poles, the solution of Pole 2 is preferred. Indeed, which pole solution is true requires more observations, even observations with other techniques (e.g., imaging, occultation, or radar).

In order to understand the inversion results intuitively, the modeled brightnesses of 2005 UD corresponding to the Pole 2 solution are shown

in Fig. 1 together with the observations. Most observed brightnesses are fitted well by the modeled brightness, but some data (e.g., data obtained on Oct. 10, 2018) are not. This minor caveat may be due to the fast sky-plane motion of the asteroid, resulting in a low quality of photometric data due to the elongated image of the asteroid.

3.3. Phase curve inversion

The photometric phase curve of an asteroid shows the observed brightness variation as a function of the solar phase angle. Here, we use the H , G_1 , G_2 phase function (Muinonen et al. (2010)), adopted by IAU in 2012, to fit the calibrated photometric data of 2005 UD. The basic equation for phase curve inversion is

$$\begin{aligned} 10^{-0.4V(\alpha)} &= a_1\phi_1(\alpha) + a_2\phi_2(\alpha) + a_3\phi_3(\alpha) \\ &= 10^{-0.4H}[G_1\phi_1(\alpha) + G_2\phi_2(\alpha) + (1 - G_1 - G_2)\phi_3(\alpha)]. \end{aligned} \quad (8)$$

The source code for H , G_1 , G_2 phase curve inversion is openly available.⁴ In practice, the phase curve inversion is carried out on the disk-integrated brightnesses in flux (see Eq. (8)), the linear parameters a_1 , a_2 , and a_3 are actually fitted, then the parameters H , G_1 , and G_2 are calculated using Eq.

⁴ <http://h152.it.helsinki.fi/HG1G2/>.

19 in Muinonen et al. (2010). The functions $\phi_{1,2,3}(\alpha)$ are basis functions expressed in cubic splines with the interpolation grid of phase angles of ($0^\circ, 0.3^\circ, 1^\circ, 2^\circ, 4^\circ, 8^\circ, 15^\circ, 30^\circ, 60^\circ, 90^\circ, 120^\circ$, and 150°). The detailed values are available in Tables 3 and 4 in Muinonen et al. (2010).

For the phase curve inversion of 2005 UD, the mean values of the dense lightcurves and ZTF data are used to fit the H, G_1, G_2 function with the MCMC method. In the MCMC simulation, the a posteriori distributions of parameters are derived by the Metropolis-Hastings algorithm from the Gaussian proposal probability densities of the parameters. Fig. 7 shows the joint distributions of the three parameters. Using $1 - \sigma$ limits of the distributions, we obtain $H = 17.22^{+0.03}_{-0.03}$ mag, $G_1 = 0.61^{+0.02}_{-0.02}$, $G_2 = -0.006^{+0.006}_{-0.006}$. The best-fit model to the photometric data is displayed in Fig. 2. From the best-fit values of G_1 and G_2 , 2005 UD is likely to be a C-type asteroid according to the suggestion in Shevchenko et al. (2016).

4. Summary

In order to study the near-Earth asteroid 2005 UD, we carried out 11 nights of photometric observations with a 30-cm telescope at the Corona borealis Observatory in Ali, Tibet, China. Combining our 11 lightcurves with the 3 lightcurves from the MPC database, the spin and shape parameters of 2005 UD are estimated with the Lommel-Seeliger ellipsoid method. Two candidate pole solutions, Pole 1 ($72^\circ.6^{+4.2}_{-7.3}$, $-84^\circ.6^{+6.2}_{-2.1}$) and Pole 2 ($285^\circ.8^{+1.1}_{-5.3}$, $-25^\circ.8^{+5.3}_{-12.5}$), are derived. Comparing the distributions of spin parameters, we prefer Pole 2, since it gives more concentrated distributions. The axial ratios of the ellipsoid corresponding to Pole 2 are $b/a = 0.76^{+0.01}_{-0.01}$, $c/a = 0.40^{+0.03}_{-0.01}$. The spin period is $5.23403^{+0.00004}_{-0.00001}$ h.

The distribution of the pole latitude (see Figs. 5 and 6) is wider than that of the pole longitude. This is due to a small span of the aspect angles of the photometric data. So more photometric observations are necessary for improving the pole orientation, especial in latitude.

Our group also focuses on the physical studies of another PGC member, (3200) Phaethon. Our group gives a pair of poles of ($95^\circ.9, -20^\circ.4$) and ($311^\circ.2, -23^\circ.6$) (a paper is in prepared). Investigating published pole solutions of Phaethon, the pole 2 solutions are mainly located around three directions: (a) ($276^\circ, -15^\circ$) (Krugly et al. (2002)), (b) ($311^\circ.2, -23^\circ.6$) (our group's work) and (c) ($319^\circ, -39^\circ$) (Hanuš et al. (2016)). If considering the uncertainty of the pole solutions, the pole 2 of 2005 UD appears to align with that of Phaethon's, especial close to our group's results. We think this evidence supports that 2005 UD probably originated via a collision or rotational fission from Phaethon's parent body, resembling the case of the Koronis family (Slivan (2002)).

Combining the mean magnitudes of the dense lightcurves and the ZTF data, we have fitted the photometric phase curve of 2005 UD with the three parameter H, G_1, G_2 phase function. The parameters H, G_1 and G_2 are as follows: $17.22^{+0.03}_{-0.03}$ mag, $0.61^{+0.02}_{-0.02}$, $-0.006^{+0.006}_{-0.006}$, respectively. Given these values of the parameters, the phase integral parameter q , photometric phase coefficient k and the enhancement factor ζ are estimated to be 0.2508, -1.9224 , and 1.6642 using equations 22, 23 and 24 in Muinonen et al. (2010).

Based on the new derived H value and the relationship of the diameter and albedo ($D = \frac{1329}{\sqrt{p_v}} 10^{-0.2H}$) (Bowell et al. (1989)), the equivalent diameter D of 2005 UD is estimated to be 1.28 ± 0.02 km using its new derived albedo of 0.14 (Masiero et al. (2019)), which is slightly larger than the previously estimated value of 1.2 ± 0.4 km (Masiero et al. (2019)).

CRedit authorship contribution statement

J.-N. Huang: Data reduction, Formal analysis, Writing - original draft. **K. Muinonen:** Software, Writing - original draft. **T. Chen:** Observation. **X.-B. Wang:** Software, Writing - original draft.

Declaration of competing interest

The authors declare that they have no known competing financial interests or personal relationships that could have appeared to influence the work reported in this paper.

Acknowledgements

The research has been funded by the National Natural Science Foundation of China (Grant Nos. 11073051 and 11673063) and the Academy of Finland (Grant No. 325805). The research has made use of the NASA/IPAC Infrared Science Archive, which is funded by the National Aeronautics and Space Administration and operated by the California Institute of Technology. The work includes data from the Asteroid Terrestrial-impact Last Alert System (ATLAS) project. ATLAS is primarily funded to search for near-Earth asteroids through NASA grants NN12AR55G, 80NSSC18K0284, and 80NSSC18K1575; byproducts of the near-Earth-object search include images and catalogs from the survey area. The ATLAS science products have been made possible through the contributions of the University of Hawaii Institute for Astronomy, the Queen's University Belfast, the Space Telescope Science Institute, and the South African Astronomical Observatory.

Appendix A. Supplementary data

Supplementary data to this article can be found online at <https://doi.org/10.1016/j.pss.2020.105120>.

References

- Bellm, E.C., Kulkarni, S.R., Graham, M.J., Dekany, R., Smith, R.M., Riddle, R., Masci, F.J., Helou, G., Prince, T.A., Adams, S.M., Barbarino, C., Barlow, T., Bauer, J., Beck, R., Belicki, J., Biswas, R., Blagorodnova, N., Bodewits, D., Bolin, B., Brinell, V., Brooke, T., Bue, B., Bulla, M., Burruss, R., Cenko, S.B., Chang, C.K., Connolly, A., Coughlin, M., Cromer, J., Cunningham, V., De, K., Delacroix, A., Desai, V., Duev, D.A., Eadie, G., Farnham, T.L., Feeney, M., Feindt, U., Flynn, D., Franckowiak, A., Frederic, S., Fremling, C., Gal-Yam, A., Gezari, S., Giomi, M., Goldstein, D.A., Golkhou, V.Z., Goobar, A., Groom, S., Hacquins, E., Hale, D., Henning, J., Ho, A.Y.Q., Hover, D., Howell, J., Hung, T., Huppenkothen, D., Imel, D., Ip, W.H., Ivezic, Z., Jackson, E., Jones, L., Juric, M., Kasliwal, M.M., Kaspi, S., Kaye, S., Kelley, M.S.P., Kowalski, M., Kramer, E., Kupfer, T., Landry, W., Laher, R.R., Lee, C.D., Lin, H.W., Lin, Z.Y., Lunnan, R., Giomi, M., Mahabal, A., Mao, P., Miller, A.A., Monkewitz, S., Murphy, P., Ngeow, C.C., Nordin, J., Nugent, P., Ofek, E., Patterson, M.T., Penprase, B., Porter, M., Rauch, L., Rebbapragada, U., Reiley, D., Rigault, M., Rodriguez, H., van Roestel, J., Rusholme, B., van Santen, J., Schulze, S., Shupe, D.L., Singer, L.P., Soumagnac, M.T., Stein, R., Surace, J., Sollerman, J., Szkody, P., Taddia, F., Terek, S., Van Sistine, A., van Velzen, S., Vestrand, W.T., Walters, R., Ward, C., Ye, Q.Z., Yu, P.C., Yan, L., Zolkower, J., 2019. The Zwicky transient facility: system overview, performance, and first results. *Publ. Astron. Soc. Pac.* 131, 018002 <https://doi.org/10.1088/1538-3873/aaecbe> arXiv:1902.01932.
- Bowell, E., Hapke, B., Domingue, D., Lumme, K., Peltoniemi, J., Harris, A.W., 1989. *Application of photometric models to asteroids*. In: Binzel, R.P., Gehrels, T., Matthews, M.S. (Eds.), *Asteroids II*, pp. 524–556.
- Collier Cameron, A., Pollacco, D., Street, R.A., Lister, T.A., West, R.G., Wilson, D.M., Pont, F., Christian, D.J., Clarkson, W.I., Enoch, B., Evans, A., Fitzsimmons, A., Haswell, C.A., Hellier, C., Hodgkin, S.T., Horne, K., Irwin, J., Kane, S.R., Keenan, F.P., Norton, A.J., Parley, N.R., Osborne, J., Ryans, R., Skillen, I., Wheatley, P.J., 2006. A fast hybrid algorithm for exoplanetary transit searches. *Mon. Not. Roy. Astron. Soc.* 373, 799–810. <https://doi.org/10.1111/j.1365-2966.2006.11074.x> arXiv:astro-ph/0609418.
- Dymock, R., Miles, R., 2009. A method for determining the V magnitude of asteroids from CCD images. *J. Br. Astron. Assoc.* 119, 149–156 arXiv:1006.4017.
- Hanus, J., Durech, J., Oszkiewicz, D.A., Behrend, R., Carry, B., Delbo, M., Adam, O., Afonina, V., Anquetin, R., Antonini, P., Arnold, L., Audejean, M., Aurard, P., Bachschmidt, M., Baduel, B., Barbotin, E., Barroy, P., Baudouin, P., Berard, L., Berger, N., Bernasconi, L., Bosch, J.G., Bouley, S., Bozhinova, I., Brinsfield, J., Brunetto, L., Canaud, G., Caron, J., Carrier, F., Casalnuovo, G., Casulli, S., Cerda, M., Chalamet, L., Charbonnel, S., Chinaglia, B., Cikota, A., Colas, F., Coliac, J.F., Collet, A., Coloma, J., Conjat, M., Conseil, E., Costa, R., Crippa, R., Cristofanelli, M., Damerjji, Y., Debackère, A., Decock, A., Déhais, Q., Déléage, T., Delmelle, S., Demeautis, C., Drózd, M., Dubos, G., Dulcamara, T., Dumont, M., Durkee, R., Dymock, R., Escalante del Valle, A., Esseiva, N., Esseiva, R., Esteban, M., Faucher, T., Fauerbach, M., Fauvaud, M., Fauvaud, S., Forné, E., Fournel, C., Fradet, D., Garlitz, J., Gerteis, O., Gillier, C., Gillon, M., Giraud, R., Godard, J.P., Goncalves, R., Hamanowa, H., Hamanowa, H., Hay, K., Hellmich, S., Heterier, S., Higgins, D., Hirsch, R., Hodosan, G., Hren, M., Hygate, A., Innocent, N., Jacquinet, H., Jawahar, S., Jehin, E., Jerosimic, L., Klotz, A., Koff, W., Korlevic, P.,

- Kosturkiewicz, E., Krafft, P., Krugly, Y., Kugel, F., Labrevoir, O., Lecacheux, J., Lehký, M., Leroy, A., Lesquerbault, B., Lopez-Gonzales, M.J., Lutz, M., Mallecot, B., Manfroid, J., Manzini, F., Marciniak, A., Martin, A., Modave, B., Montaigut, R., Montier, J., Morelle, E., Morton, B., Mottola, S., Naves, R., Nomen, J., Oey, J., Ogloza, W., Paiella, M., Pallares, H., Peyrot, A., Pilcher, F., Pirenne, J.F., Piron, P., Polińska, M., Polotto, M., Poncy, R., Previt, J.P., Reignier, F., Renauld, D., Ricci, D., Richard, F., Rinner, C., Risoldi, V., Robilliard, D., Romeuf, D., Rousseau, G., Roy, R., Ruthroff, J., Salom, P.A., Salvador, L., Sanchez, S., Santana-Ros, T., Scholz, A., Séné, G., Skiff, B., Sobkowiak, K., Sogorb, P., Soldán, F., Spiridakis, A., Splanska, E., Sposetti, S., Starkey, D., Stephens, R., Stiepen, A., Stoss, R., Strajnic, J., Teng, J.P., Tumolo, G., Vagnozzi, A., Vanouryve, B., Vugnon, J.M., Warner, B.D., Waucomont, M., Wertz, O., Winiarski, M., Wolf, M., 2016. New and updated convex shape models of asteroids based on optical data from a large collaboration network. *Astron. Astrophys.* 586, A108. <https://doi.org/10.1051/0004-6361/201527441> arXiv:1510.07422.
- Jewitt, D., 2013. Properties of near-sun asteroids. *Astron. J.* 145, 133. <https://doi.org/10.1088/0004-6256/145/5/133>, arXiv:1303.2415.
- Jewitt, D., Hsieh, H., 2006. Physical observations of 2005 UD: a mini-Phaethon. *Astron. J.* 132, 1624–1629. <https://doi.org/10.1086/507483>.
- Kasuga, T., Jewitt, D., 2008. Observations of 1999 YC and the breakup of the Geminid stream parent. *Astron. J.* 136, 881–889. <https://doi.org/10.1088/0004-6256/136/2/881>, arXiv:0805.2636.
- Kinoshita, D., Ohtsuka, K., Sekiguchi, T., Watanabe, J., Ito, T., Arakida, H., Kasuga, T., Miyasaka, S., Nakamura, R., Lin, H.C., 2007. Surface heterogeneity of 2005 UD from photometric observations. *Astron. Astrophys.* 466, 1153–1158. <https://doi.org/10.1051/0004-6361:20066276>.
- Krugly, Y., Belskaya, I.N., Mykhailova, S.S., Donchev, Z., Inasaridze, R.Y., Sergeyev, A.V., Slyusarev, I.G., Shevchenko, V.G., Chiorny, V.G., Rummyantsev, V.V., Novichonok, A.O., Ayvazian, V., Kapanadze, G., Kvaratskhelia, O.I., Bonev, T., Borisov, G., Molotov, I.E., Voropaev, V.A., 2019. Photometry and polarimetry of near-Earth asteroids (3200) Phaethon and (155140) 2005 UD. In: EPSC-DPS Joint Meeting 2019. EPSC-DPS2019–1989.
- Krugly, Y.N., Belskaya, I.N., Shevchenko, V.G., Chiorny, V.G., Velichko, F.P., Mottola, S., Erikson, A., Hahn, G., Nathues, A., Neukum, G., Gaftonyuk, N.M., Dotto, E., 2002. The near-earth objects follow-up program. IV. CCD Photometry in 1996–1999. *Icarus* 158, 294–304. <https://doi.org/10.1006/icar.2002.6884>.
- Laher, R.R., Surace, J., Grillmair, C.J., Ofek, E.O., Levitan, D., Sesar, B., van Eyken, J.C., Law, N.M., Helou, G., Hamam, N., Masci, F.J., Mattingly, S., Jackson, E., Hacoceans, E., Mi, W., Groom, S., Teplitz, H., Desai, V., Hale, D., Smith, R., Walters, R., Quimby, R., Kasliwal, M., Hoeshe, A., Bellm, E., Barlow, T., Waszczak, A., Prince, T.A., Kulkarni, S.R., 2014. IPAC Image Processing and Data Archiving for the Palomar Transient Factory, vol. 126. Publications of the Astronomical Society of the Pacific, p. 674. <https://doi.org/10.1086/677351> arXiv:1404.1953.
- Masiero, J.R., Wright, E.L., Mainzer, A.K., 2019. Thermophysical modeling of NEOWISE observations of DESTINY⁺ targets Phaethon and 2005 UD. *Astron. J.* 158, 97. <https://doi.org/10.3847/1538-3881/ab31a6> arXiv:1907.04518.
- Muinenen, K., Belskaya, I.N., Cellino, A., Delbò, M., Levasseur-Regourd, A.C., Penttilä, A., Tedesco, E.F., 2010. A three-parameter magnitude phase function for asteroids. *Icarus* 209, 542–555. <https://doi.org/10.1016/j.icarus.2010.04.003>.
- Muinenen, K., Wilkman, O., Cellino, A., Wang, X., Wang, Y., 2015. Asteroid lightcurve inversion with Lommel-Seeliger ellipsoids. *Planet. Space Sci.* 118, 227–241. <https://doi.org/10.1016/j.pss.2015.09.005>.
- Ofek, E.O., Laher, R., Law, N., Surace, J., Levitan, D., Sesar, B., Hoeshe, A., Poznanski, D., van Eyken, J.C., Kulkarni, S.R., Nugent, P., Zolkower, J., Walters, R., Sullivan, M., Agüeros, M., Bildsten, L., Bloom, J., Cenko, S.B., Gal-Yam, A., Grillmair, C., Helou, G., Kasliwal, M.M., Quimby, R., 2012. The Palomar Transient Factory Photometric Calibration, vol. 124. Publications of the Astronomical Society of the Pacific, p. 62. <https://doi.org/10.1086/664065> arXiv:1112.4851.
- Ohtsuka, K., Sekiguchi, T., Kinoshita, D., Watanabe, J.I., Ito, T., Arakida, H., Kasuga, T., 2006. Apollo asteroid 2005 UD: split nucleus of (3200) Phaethon? *Astron. Astrophys.* 450, L25–L28. <https://doi.org/10.1051/0004-6361:200600022>.
- Shevchenko, V.G., Belskaya, I.N., Muinenen, K., Penttilä, A., Krugly, Y.N., Velichko, F.P., Chiorny, V.G., Slyusarev, I.G., Gaftonyuk, N.M., Tereschenko, I.A., 2016. Asteroid observations at low phase angles. IV. Average parameters for the new H, G₁, G₂ magnitude system. *Planet. Space Sci.* 123, 101–116. <https://doi.org/10.1016/j.pss.2015.11.007>.
- Slivan, S.M., 2002. Spin vector alignment of Koronis family asteroids. *Nature* 419, 49–51. <https://doi.org/10.1038/nature00993>.
- Tamuz, O., Mazeh, T., Zucker, S., 2005. Correcting systematic effects in a large set of photometric light curves. *Mon. Not. Roy. Astron. Soc.* 356, 1466–1470. <https://doi.org/10.1111/j.1365-2966.2004.08585.x> arXiv:astro-ph/0502056.
- Wang, X.B., Gu, S.H., Collier Cameron, A., Tan, H.B., Hui, H.K., Kwok, C.T., Yeung, B., Leung, K.C., 2013. The refined physical parameters of transiting exoplanet system HAT-P-24. *Res. Astron. Astrophys.* 13, 593–603. <https://doi.org/10.1088/1674-4527/13/5/010>.
- Warner, B.D., Stephens, R.D., 2019. Near-earth asteroid lightcurve analysis at the center for solar system studies: 2018 september–december. *Minor Planet Bull.* 46, 144–152.